

This item was submitted to Loughborough's Institutional Repository (<https://dspace.lboro.ac.uk/>) by the author and is made available under the following Creative Commons Licence conditions.



For the full text of this licence, please go to:  
<http://creativecommons.org/licenses/by-nc-nd/2.5/>

# Effects of bandwidth limitations on the localized state distribution calculated from transient photoconductivity data

D. P. Webb

*Department of Electronic Engineering, City University of Hong Kong, Tat Chee Avenue, Kowloon, Hong Kong*

C. Main and S. Reynolds

*School of Engineering, University of Abertay Dundee, Dundee DD1 1HG, Scotland, United Kingdom*

Y. C. Chan<sup>a)</sup> and Y. W. Lam

*Department of Electronic Engineering, City University of Hong Kong, Tat Chee Avenue, Kowloon, Hong Kong*

S. K. O'Leary

*Department of Electrical, Computer, and Systems Engineering, Rensselaer Polytechnic Institute, Troy, New York 12180-3590*

(Received 8 September 1997; accepted for publication 26 January 1998)

The possible effects of experimental bandwidth limitation on the accuracy of the energy distribution of the density of localized states (DOS) calculated from transient photoconductivity data by the Fourier transform method is examined. An argument concerning the size of missing contributions to the numerical Fourier integrals is developed. It is shown that the degree of distortion is not necessarily large even for relatively small experimental bandwidths. The density of states calculated from transient photodecay measurements in amorphous arsenic triselenide is validated by comparing with modulated photocurrent data. It is pointed out that DOS distributions calculated from transient photoconductivity data at a high photoexcitation density are valid under certain conditions. This argument is used to probe the conduction band tail in undoped *a*-Si:H to energies shallower than 0.1 eV below the mobility edge. It is concluded that there is a deviation in the DOS from exponential at about 0.15 eV below the mobility edge. © 1998 American Institute of Physics. [S0021-8979(98)03409-4]

## I. INTRODUCTION

Transient photoconductive techniques have long been an attractive prospect as a probe of the localized density of states distribution (DOS) in amorphous photoconducting materials. The shape of the time resolved transient photocurrent (TPC) decay is evidently controlled by trapping and release from localized states, and therefore much effort has gone into attempts to extract information on the DOS from the data.<sup>1-4</sup> This has proved difficult, because the state of the transient carrier distribution at any moment depends on the history of the decay. Thus the transient photocurrent  $\delta I(t)$  at time  $t$  cannot in a generally true way be related to the density of localized states  $g(E)dE$  at energy  $E$  in the mobility gap.

The problem of relating current to the DOS is far more tractable in the frequency domain. In the modulated photocurrent (MPC) experiment, photocarriers are generated by a light source the intensity of which is sinusoidally modulated. The resulting photocurrent has a sinusoidal alternating component (ac) which in general is phase shifted with respect to the light source modulation. Brüggemann *et al.*<sup>5</sup> devised a method of calculating  $g(E_\omega)$ , at a unique energy  $E_\omega$  for each modulation angular frequency  $\omega$ , from the ac magnitude and phase. Hattori *et al.*<sup>6</sup> further refined the method.

MPC has the disadvantages of being limited in the modulation frequency range that can be covered, and also having an intrinsic steady component (optical bias) in the photogeneration rate variation with time. Both these factors limit the energy range in the DOS which can be covered. The Fourier transform of transient photocurrent (FTTPC) method<sup>7</sup> allows use of the frequency domain DOS calculation methods with time domain TPC data by the use of a Fourier transform. The effective frequency range of the hybrid is very wide and optical bias can be eliminated. TPC is also experimentally simpler to setup than MPC, for which great attention must be paid to eliminating phase error.

The use of a Fourier transform introduces other problems, chief among which is that the calculated transform is only an approximation to the true frequency response, because the whole of the time domain transient response is not sampled. In practice "the whole" would mean sampling at times short enough to see the pretrapping transient photocurrent, i.e., the photocurrent when all of the transient carrier packet still occupies extended states. Trapping occurs at around  $10^{-12}$  s in *a*-Si:H, but the shortest time resolvable by digital sampling electronics is about  $10^{-9}$  s. The resultant degree of error in the calculated DOS is not necessarily serious, but does depend on the shape of the transient photodecay, weakening the generality of applicability of the

<sup>a)</sup>Electronic mail: eeychan@cityu.edu.hk

FTTPC method. Another limitation is the requirement for a small, and hence more difficult to measure TPC signal magnitude, so that the TPC response is linear and the Fourier transform is valid. Standard fast Fourier transform (FFT) algorithms cannot be used for the Fourier transform, since the signal to be operated upon can extend over more than ten orders of magnitude in current and time. However, it turns out that the calculation procedure required is straightforward.

This work is a discussion of the limits imposed by the problems outlined above, and other considerations, on the use of the FTTPC method to obtain a localized density of states distribution, with particular reference to *a*-Si:H.

## II. THEORY

A slightly improved version of the FTTPC calculation method in Ref. 7 is briefly reviewed here. The transient photocurrent decay  $\delta I(t)$  is considered to be the response to an impulse photogeneration producing a density  $\delta G$  electron-hole pairs. The response to unit impulse is thus  $h(t) = \delta I(t)/\delta G$  for small enough  $\delta G$ . The Fourier transform of  $h(t)$  is the complex transfer function  $H(\omega)$ . Experimental TPC data consists of a set of  $M$  current-time values  $\delta I(t_k), t_k$ . An approximation to  $H(\omega)$  is calculated as the *exact* Fourier transform of a linear spline interpolated function defined by the  $\delta I(t_k), t_k$ , i.e.,

$$\Re\{H(\omega_n)\} \approx a(\omega_n) = (\delta G \omega_n)^{-1} \sum_{k=2}^M \left\{ \frac{s_k}{\omega_n} [\cos(\omega_n t_k) - \cos(\omega_n t_{k-1})] + [\delta I(t_k) \sin(\omega_n t_k) - \delta I(t_{k-1}) \sin(\omega_n t_{k-1})] \right\}, \quad (1)$$

$$\Im\{H(\omega_n)\} \approx b(\omega_n) = (\delta G \omega_n)^{-1} \sum_{k=2}^M \left\{ \frac{s_k}{\omega_n} [\sin(\omega_n t_k) - \sin(\omega_n t_{k-1})] - [\delta I(t_k) \cos(\omega_n t_k) - \delta I(t_{k-1}) \cos(\omega_n t_{k-1})] \right\}, \quad (2)$$

where  $s_k = [\delta I(t_k) - \delta I(t_{k-1})]/(t_k - t_{k-1})$ , and the  $\omega_n$  are arbitrarily selected. Oscillation in  $a$  and  $b$  at small  $\omega_n$  is avoided by premultiplying the  $\delta I(t_k)$  by a windowing function that causes the values to tend smoothly to zero at long time.

Values of the DOS function  $g(E_n)$  may then be computed as follows:

$$g(E_n) = \frac{2e\mu\epsilon A}{C_n \pi kT} \left\{ \frac{\sin \phi(\omega_n)}{|H(\omega_n)|} - \omega_n \right\}, \quad (3)$$

$$E_c - E_n = kT \ln(\nu/\omega_n), \quad (4)$$

where  $H = |H|e^{-i\phi}$ ,  $e$  is the electronic charge,  $\mu$  is the free electron mobility,  $\epsilon$  is the electric field,  $A$  is the conduction path cross section,  $C_n$  is the capture coefficient,  $\nu$  is the attempt to escape frequency for localized states,  $k$  is Boltzmann's constant,  $T$  is the temperature,  $E_c$  is the energy of the conduction band mobility edge, and the majority carrier is taken to be electrons. A similar expression may be devised for hole transport. In practice the  $\omega_n$  term in the curly brackets in Eq. (3) may usually be ignored. The DOS is calculated for values of  $\omega_n$  in the range  $1/t_{\max} < \omega_n < 1/t_{\min}$  and  $g(E_n), E_n$  values affected by the windowing function referred to above are removed.

Equation (3) is based upon an approximation in the MPC analysis for a sensitivity function relating the ac occupation of extended states to the density of localized states over a range in energy. The function is peaked at the energy  $E_n$  defined by Eq. (4), and Eq. (3) is obtained by approximating this sensitivity function by a delta function of the same area situated at  $E_n$ . The effect of the approximation is to blur features in the reproduced DOS, for example a narrow band of localized states is reproduced at the correct energy but

with a  $2kT$  spread. A conduction band tail of exponential slope  $kT_c < kT$  is reproduced as having a slope of around  $kT$ .

The Hattori *et al.*<sup>6</sup> MPC DOS calculation method may also be used with  $H(\omega)$  as follows:

$$g(E_n) \approx \frac{e\mu\epsilon A}{C_n kT} \frac{d}{d[\ln(\omega)]} \left\{ \frac{\cos(\phi)}{|H(\omega_n)|} \right\}. \quad (5)$$

The energy scale is still given by Eq. (4). The above equation has the advantage of having a sharper associated sensitivity function, with tails of slope  $kT/2$ , thereby reducing the blurring of features in the DOS. The disadvantage is that a numerical differential must be calculated, which emphasizes experimental noise. In this work Eq. (3) is used to calculate the DOS unless otherwise noted.

## III. EXPERIMENTAL METHODS

TPC experiments were performed on 1- $\mu\text{m}$ -thick films of undoped amorphous silicon produced by plasma-enhanced chemical-vapor deposition (PECVD) at the Universities of Stuttgart, Germany, and Shantou, China. The PECVD method used at the University of Shantou is described in Ref. 8. Coplanar aluminium electrodes of gap 0.5 mm were deposited on the surface of the samples. The TPC measurements were made using a field voltage of 300 V. A nitrogen pumped dye laser was used to produce photogeneration pulses of width 3 ns, at wavelengths of 640 nm for the Stut-

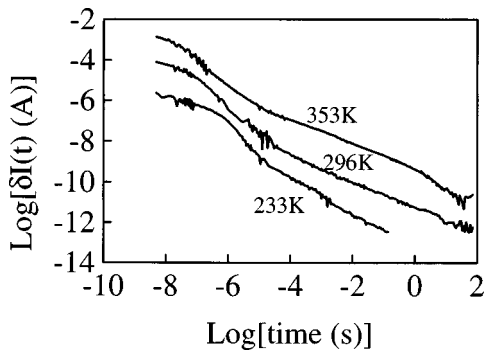


FIG. 1. Transient photocurrent decays measured in the Stuttgart *a*-Si:H at three different temperatures. The curves for 233 and 353 K have been shifted by a decade downwards and upwards, respectively, for clarity.

tgart material, and 595 nm for the Shantou material. Special purpose wideband current mode operational amplifier circuits were used to sample  $\delta I(t)$ , the decay curves presented here being multichannel averaged composites of the response at several bandwidths. Time was allowed for relaxation between each laser firing. For more details of the experimental setup see Ref. 9.

#### IV. DEEP STATES IN *a*-Si:H

Figure 1 shows TPC measured in the Stuttgart sample<sup>10</sup> at three temperatures, for a photogeneration pulse  $\delta G = 10^{16} \text{ cm}^{-3}$  which is in the linear response regime. The shape of the decays is typical for such measurements in *a*-Si:H. There is a short time, relatively nondispersive region, followed by a steep fall and then a long time power law decay. The transition between the nondispersive region and the steep fall moves to progressively longer times with decreasing temperature while the magnitude of the current in the nondispersive region decreases.

The results of application of the FTTPC method using Eq. (3) and (4) to the above data are shown in Fig. 2. A DOS consisting of a steep exponential tail and a deep energy broad bump centered at about 0.65 eV below  $E_c$  is mapped out. Note that the DOS distribution calculated for the 353 K data using the Brüggemann *et al.* equation, Eq. (3), produces a shallower tail slope than for the 233 K data. This is a result of the  $kT$  blurring effect alluded to above. The greater selec-

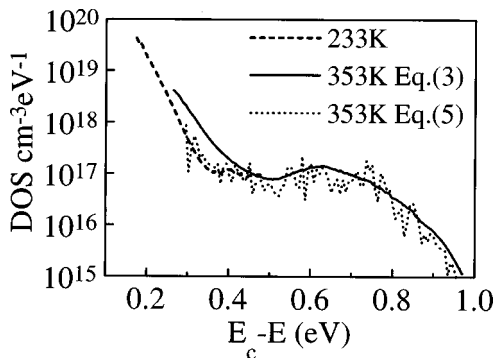


FIG. 2. Density of states distribution calculated from data in Fig. 1. The 353 K distribution has been calculated using both Eqs. (3) and (5).

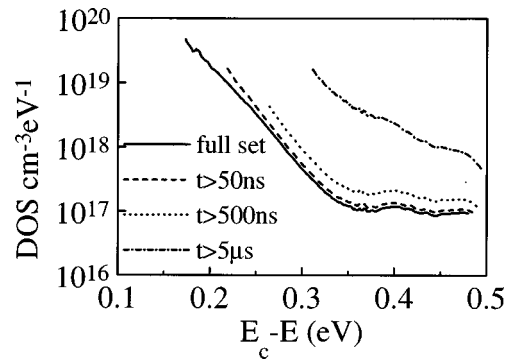


FIG. 3. Density of states distributions calculated from subsets of the 233 K data set. In each subset data points for times shorter than that indicated have been removed.

tivity of the Hattori *et al.* equation, Eq. (5), produces a better match between tail slopes, but the noise enhancement due to differentiation is also evident.

The scaling parameters used are  $\mu = 10 \text{ cm}^2(\text{Vs})^{-1}$ ,  $\nu = 10^{12} \text{ s}^{-1}$ , and  $C_n = 10^{-8} \text{ cm}^3 \text{ s}^{-1}$ . From detailed balance  $\nu = C_n N_c$ , where the effective density of states at the band edge  $N_c$  is  $kT$  times the actual density  $G_c$ . This explicit temperature dependence in  $N_c$ , however, is balanced by the unknown temperature dependence of  $\mu$ . We find that a reasonable match between the DOS distributions for data measured at differing temperatures is obtained using the temperature independent values quoted above.<sup>11</sup> Experimental support for the value of  $\nu$  is given below.

The reproduced shape of the deep energy bump can be shown to be dependent on the relationship between the magnitudes of the contribution to the Fourier integral from the short time nondispersive region and the long time power law decay in the data sets of Fig. 1. In Fig. 3 DOS distributions calculated from subsets of the 233 K data set are shown. For each subset all data points for times shorter than a chosen limit are removed. It can be seen that the shape of the deep energy distribution is not affected until the whole of the short time nondispersive region is removed, i.e., all data points for  $t < 5 \mu\text{s}$ . Two general conclusions concerning the Fourier transform method for calculating the DOS may be drawn from this behavior. First, even with a limited experimental bandwidth the method can still produce the correct DOS. Second, given that transient photocurrent decays are of monotonically decreasing character, the question of whether the bandwidth limitation distorts the calculated DOS becomes the question of whether there is a significantly large missing contribution to the Fourier transform due to there being a very much higher current at times shorter than the experimental time window.

These points may be elucidated by consideration of the transient photocharge, i.e., the cumulative integral of the transient photocurrent, see Fig. 4. The integral of the 296 K data exhibits an initial rise, a plateau after about  $0.5 \mu\text{s}$ , and a final rise beginning at about 50 ms. This structure reflects the dominance of the contribution to the integral from the nondispersive short time current in the TPC decay. Although the short time region in the TPC decay ends at about 100 ns, the value of the cumulative integral remains at the value of

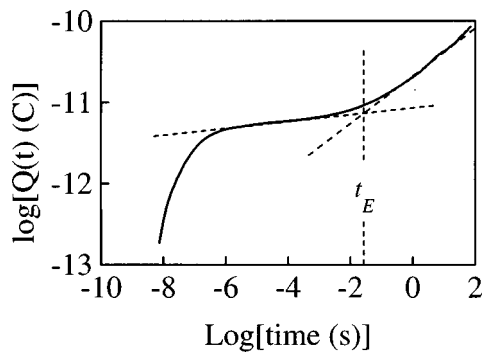


FIG. 4. Photocharge (cumulative integral) plot of the 296 K decay of Fig. 1. The time  $t_E$  is the emission time from deep states.

the integral of the short time region until the final rise at 50 ms. The nondispersive short time region in the TPC decay similarly dominates the Fourier integrals.

Physically, the shape of the transient photocharge plot reflects the deep trapping and release of charge.<sup>12</sup> The initial rise corresponds to multiple trapping transport with the transient carrier packet being repeatedly trapped and released by the shallow energy conduction band tail localized state distribution. At about 100 ns the majority of carriers become trapped in deep states, so that they no longer contribute to conduction and so the transient photocharge plot plateaus out. Only when the deeply trapped electrons are released at about 50 ms do they contribute to conduction again. The final rise in the transient photocharge plot therefore reflects the release time from deep traps. The variation of this release time with temperature may be used in an Arrhenius plot [ $\ln(t)$  vs  $1/T$ ] to obtain values for the attempt to escape frequency  $\nu$  and the energy depth of the deep traps. For the Stuttgart material the values obtained in this way were  $1.3 \times 10^{12} \text{ s}^{-1}$  and 0.63 eV below  $E_c$ , respectively.

## V. AMORPHOUS ARSENIC TRISELENIDE

Amorphous arsenic triselenide,  $a\text{-As}_2\text{Se}_3$ , is an interesting material for which to assess the accuracy of a DOS calculated by FTTPC. The model used to explain the steady state photocurrent dependence on photogeneration rate TPC in  $a\text{-As}_2\text{Se}_3$ <sup>13,14</sup> places recombination centers at 0.66 eV above the valence band mobility edge. However, TPC decays in the material are accurate power laws over many orders of time, which in the past has been interpreted as corresponding to a broad exponential band tail with no feature where the recombination centers should be. The majority carrier is holes, so that the valence band tail is probed.

As we have seen with amorphous silicon, such power law decays do not necessarily correspond to a featureless band tail. The bandwidth of TPC measurements on  $a\text{-As}_2\text{Se}_3$  is generally much smaller than for  $a\text{-Si:H}$  measurements, because the magnitude of the signal is much smaller. We find that the current for  $t < 1 \mu\text{s}$  cannot be sampled. If there is a missing large contribution to the Fourier integrals from the unsampled region of the signal then the exponential DOS calculated from such data would be incorrect. One way to assess whether there is such a missing contribution is to compare the DOS calculated by FTTPC, and from direct

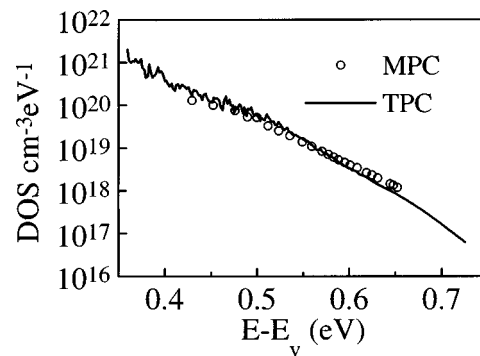


FIG. 5. Density of states distribution in a sample of  $a\text{-As}_2\text{Se}_3$  calculated from transient photocurrent and modulated photocurrent experiments.

sampling of the frequency domain response by modulated photocurrent measurements. The match between the DOS distributions calculated from the two experiments on a single sample, shown in Fig. 5, demonstrates that there is no missing contribution and the DOS is indeed a featureless exponential. Note that the TPC data covers a wider range of energy than the MPC data, so that validating the FTTPC DOS by comparing with MPC is a useful exercise.

## VI. SHALLOW TAIL STATES IN $a\text{-Si:H}$

The general form of the localized state distribution in Fig. 2 is as expected for  $a\text{-Si:H}$ . The conduction band tail is generally taken to be at least approximately exponential. This functional form is often found to be analytically convenient but is supported by experimental evidence rather than by any generally accepted precise model for the effect of disorder on the crystalline band edge.

We apply here the FTTPC method to investigate the functional form of the conduction band tail state distribution in  $a\text{-Si:H}$ , particularly at energies shallower than about 0.15 eV below  $E_c$ . This region has not been well investigated because techniques which respond to conduction band extended states, for example inverse electron photoemission spectroscopy,<sup>15</sup> cannot follow the DOS far into the mobility gap, while techniques responsive to gap states cannot follow the DOS all the way to the mobility edge. The DOS is found to have an approximately linear energy dependence in the region of the mobility edge, so a changeover in the DOS energy dependence from exponential to linear should be observable if shallow enough energies can be probed. Longeaud and Vanderhagen<sup>16</sup> observed indications of such a changeover from low temperature time-of-flight measurements.

Figure 6<sup>17</sup> shows the low temperature TPC decays measured on the samples deposited at the University of Shantou, to probe the shallow energy DOS. Reducing the temperature allows shallower energies to be probed because the multiple trapping transport process is slowed, but for a fixed pulse generation density  $\delta G$  there is a corollary effect of reducing the transient current magnitude. This occurs because the instantaneous distribution function for transient carriers moves in favor of the trapping states, analogously to the behavior of the Fermi distribution function. In order to boost the signal to

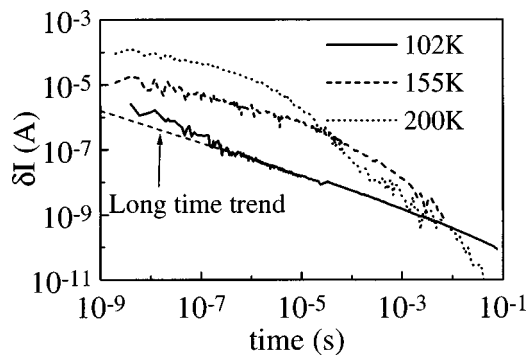


FIG. 6. Transient photocurrent measured in Shantou *a*-Si:H:  $\delta G$  for the 200 K and 155 K measurements was estimated as  $5.2 \times 10^{16} \text{ cm}^{-3}$ , for the 102 K measurement as  $5.2 \times 10^{17} \text{ cm}^{-3}$ . The trend of the long time current in the 102 K decay is marked by a line.

a resolvable level we have increased the pulse generation densities for the data of Fig. 6. Although these values of  $\delta G$  are in the nonlinear response regime for room temperature measurements, the observed response is linear over at least the shorter time portion of the experimental time window at these low temperatures. We argue that even if the response does become nonlinear at longer time, the DOS calculated from the linear response portion of the data set is correct. The power law decreasing nature of the decays means that the calculated Fourier transform is not distorted by loss of long time data. In other words the contribution to the Fourier integrals for frequency  $\omega_n$ , from  $\delta I(t)$  with  $1/t \ll \omega_n$ , may be ignored. Thus, even were  $\delta G$  to be reduced to a level at which the whole signal varied linearly with  $\delta G$ , the Fourier integrals at frequency  $\omega_n$  would take the same values as at the higher pulse generation density.

The DOS distributions calculated from the data of Fig. 6 are plotted in Fig. 7. The 155 and 200 K distributions match well, consistent with the tail slope characteristic energy  $kT_c$  of about 0.022 eV being greater than  $kT$  at both temperatures. The 102 K distribution, however, exhibits a clear deviation in shape. The discrepancy can be attributed to a *small* missing contribution to the Fourier integrals for the 155 K data set, which contribution is partially present for the 102 K set. This contribution arises from a higher current for  $t < 100$  ns in the 102 K decay, than the extrapolation to short times of the trend for  $t > 100$  ns. The trend for  $t > 100$  ns is

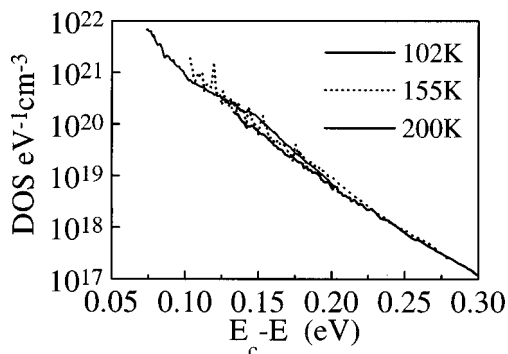


FIG. 7. Density of states distributions calculated from the data of Fig. 6. Note the deviation in the shape of the 102 K curve.

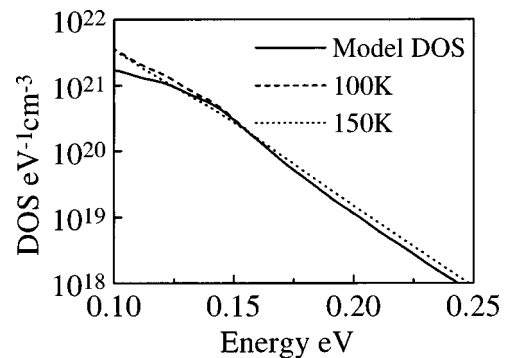


FIG. 8. Density of states distributions calculated from simulated transient photocurrent data. The data sets have been truncated at 5 ns to reproduce the effects of the experimental bandwidth limitation.

marked in Fig. 6. Such a feature should exist in the 155 K decay, but occurring at a time too short to be detected.

The high current feature is caused by a deviation in the trend of the DOS from purely exponential. This may be demonstrated by the results of the simulation shown in Fig. 8. The simulator uses a finite difference numerical technique to calculate the transient response for a given model DOS.<sup>18</sup> The input DOS consists of a linear portion extending from the band edge to a depth of 0.154 eV, followed by an exponential portion of characteristic energy  $kT_c$  0.018 eV. Decays for temperatures 100 and 150 K were simulated, then all data points for  $t < 5$  ns were removed. Finally, DOS distributions were recalculated using FTTPC from the truncated data sets. It can be seen in Fig. 8 that the 150 K recalculated DOS is almost featureless, while the 100 K curve shows pronounced structure.

We may therefore conclude that there is a changeover in the functional form of the conduction band tail from exponential to something else at about 0.15 eV below  $E_c$ . Although 0.15 eV below  $E_c$  is within the energy range of the 155 K data set, the changeover is not detected. The 102 K data allows us to detect the changeover, but not the precise functional form of the tail between 0.15 eV below  $E_c$  and  $E_c$ . This should not be seen as a failure of the FTTPC method, since the very shallow region of the DOS being investigated is at the very limit of experimental accessibility. Rather, an awareness of the sources of distortion in the FTTPC calculation has allowed us to draw a conclusion from what at first sight is contradictory data.

## VII. CONCLUSIONS

The effects of bandwidth limitations on the accuracy of the distribution of the density of localized states (DOS) with energy calculated from transient photoconductivity data by the Fourier transform method have been examined. Distortions can arise because of missing contributions to the numeric Fourier integrals from the portion of the transient decay at times too short to be sampled. It has been shown that the degree of distortion is not necessarily large even for relatively small experimental bandwidths. The size of the missing contribution to the Fourier integrals has been shown to be small for the density of states calculated from transient photodecay measurements in amorphous arsenic triselenide,

by comparing with modulated photocurrent data. It has been pointed out that DOS distributions calculated from transient photoconductivity data at high photoexcitation density are valid under certain conditions. This argument has been used to probe the conduction band tail in undoped *a*-Si:H to energies shallower than 0.1 eV below the mobility edge. The shapes of the calculated distributions have been explained using arguments about missing contributions to the Fourier integrals. It has been concluded that there is a deviation in the DOS from exponential at about 0.15 eV below the mobility edge.

#### ACKNOWLEDGMENTS

The authors would like to thank X. Lin and K. Lin at the University of Shantou for the use of their deposition facilities, and X. C. Zou and S. H. Lin for their help in sample preparation there. We would also like to thank H. D. Mohring, I. P. E. Universität Stuttgart for provision of samples.

<sup>1</sup>T. Tiedje and A. Rose, *Solid State Commun.* **37**, 49 (1981).

<sup>2</sup>J. Orenstein, M. A. Kastner, and V. A. Vaninov, *Philos. Mag. B* **46**, 23 (1982).

<sup>3</sup>J. M. Marshall, J. Berkin, and C. Main, *Philos. Mag. B* **56**, 641 (1987).

<sup>4</sup>H. Michiel, J. M. Marshall, and G. J. Adriaenssens, *Philos. Mag. B* **48**, 187 (1983).

<sup>5</sup>R. Brüggemann, C. Main, J. Berkin, and S. Reynolds, *Philos. Mag. B* **62**, 29 (1990).

<sup>6</sup>K. Hattori, Y. Adachi, M. Anzai, H. Okamoto, and Y. Hamakawa, *J. Appl. Phys.* **76**, 2841 (1994).

<sup>7</sup>C. Main, R. Brüggemann, D. P. Webb, and S. Reynolds, *Solid State Commun.* **83**, 401 (1992).

<sup>8</sup>X. Lin, H. Wang, K. Lin, Y. Yu, and S. Fu, *Thin Solid Films* **237**, 310 (1994).

<sup>9</sup>R. Brüggemann, C. Main, M. Rösch, and D. P. Webb, *Mater. Res. Soc. Symp. Proc.* **420**, 697 (1996).

<sup>10</sup>C. Main, R. Brüggemann, D. P. Webb, and S. Reynolds, *J. Non-Cryst. Solids* **164–166**, 481 (1993).

<sup>11</sup>C. Longeaud, G. Fournet, and R. Vanderhaghen, *Phys. Rev. B* **38**, 7493 (1988).

<sup>12</sup>H. Antoniadis and E. A. Schiff, *Phys. Rev. B* **46**, 9482 (1992).

<sup>13</sup>G. J. Adriaenssens, G. Seynhaeve, and S. de Greef, *J. Non-Cryst. Solids* **77–78**, 1187 (1985).

<sup>14</sup>C. Main and A. E. Owen, in *Electronic and Structural Properties of Amorphous Semiconductors*, edited by P. G. LeComber and J. Mort (Academic, London, 1972).

<sup>15</sup>R. A. Street, *Hydrogenated Amorphous Silicon* (Cambridge University Press, Cambridge, 1991).

<sup>16</sup>C. Longeaud and R. Vanderhaghen, *Philos. Mag.* **61**, 277 (1990).

<sup>17</sup>D. P. Webb, X. C. Zou, Y. C. Chan, Y. W. Lam, S. H. Lin, X. Y. Lin, K. X. Lin, S. K. O'Leary, and P. K. Lim, *Solid State Commun.* **105**, 239 (1998).

<sup>18</sup>C. Main, J. Berkin and A. Merazga, in *New Physical Problems in Electronic Materials*, edited by M. Borisov, N. Kirov, J. M. Marshall, and A. Vavrek (World Scientific, Singapore, 1991).